Geochemical fixation of rare earth elements into secondary minerals in sandstones beneath a natural fission reactor at Bangombé, Gabon

HIROSHI HIDAKA[1,2]*, JANUSZ JANECZEK[3], FRANCIS N. SKOMURSKI[4], RODNEY C. EWING[4] and FRANÇOIS GAUTHIER-LAFAYE[5]

[1]Department of Earth and Planetary Systems Science, Hiroshima University, Higashi-Hiroshima 739-8526, Japan

[2]Project Center of Multi-Isotope Research for Astro- & Geochemical Evolution (MIRAGE)
Hiroshima University, Higashi-Hiroshima 739-8526, Japan

[3]Department of Earth Sciences, University of Silesia,
ul. Bedzinska 60, PL-41-200 Sosnowiec, Poland

[4]Department of Geological Sciences,
The University of Michigan, 2355 Bonisteel Boulevard
Ann Arbor, Michigan 48109-1063, USA

[5]Ecole et Observatoire des Sciences de la Terre, UMR7517-CNRS-ULP
1 rue Blessig, 67084 Strasbourg, France

*Author to whom correspondence should be addressed (hidaka@hiroshima-u.ac.jp)

Abstract – In order to study geochemical processes for migration and fixation of fissiogenic rare earth elements (REE) in association with uranium dissolution, *in-situ* isotopic analyses using an ion microprobe were performed on U- and REE-bearing secondary minerals, such as coffinite, françoisite, uraniferous goethite, and uraninite found in a sandstone layer 30~110 cm beneath a natural fission reactor at Bangombé, Gabon. Phosphate minerals such as phosphatian coffinite and françoisite with depleted ^{235}U ($^{235}U/^{238}U$=0.00609~0.00638) contained large amount of fissiogenic light REE, while micro-sized uraninite grains in a solid bitumen aggregate have normal U isotopic values ($^{235}U/^{238}U$=0.00725) and small amount of fissiogenic REE components. The proportions of fissiogenic and non-fissiogenic REE components in four samples from the core of BAX03 vary in depth ranging from 30 cm to 130 cm beneath the reactor, which suggests mixing between fissiogenic isotopes from the reactor and non-fissiogenic isotopes from original minerals in the sandstone. Significant chemical fractionation was observed between Ce and the other REE in the secondary minerals, which shows evidence of an oxidizing atmosphere during their formation. Pb-isotopic analyses of individual minerals do not directly provide chronological information because of the disturbance of U-Pb decay system due to recent geologic alteration. However, systematic Pb-isotopic results from all of the minerals reveal the mobilization of fissiogenic isotopes, Pb and U from the reactor in association with dolerite dyke intrusion approximately 0.798 Ga ago and the formation of the secondary minerals by mixing event between 2.05 Ga-old original minerals and reactor materials due to recent alteration.

1. INTRODUCTION

Natural systems provide useful information on migration and retardation mechanisms of radioisotopes in nature and can be used to create and test models of the long-term behavior of spent nuclear fuel in the geosphere. In particular, the Oklo-Okelobond-Bangombe uranium deposits, the Republic of Gabon, central Africa, known as natural fission reactors are useful natural analogues, because large-scale fission reactions occurred spontaneously 2.0 Ga ago (Bodu et al., 1972; Neuilly et al., 1972). The behavior of the long-term geochemical behavior of actinides and fission products in the natural environment can be studied using these natural fission reactors.

The Bangombé uranium deposit is located about 30 km southeast from Oklo (Fig. 1A). In 1985, the natural fission reactor was found as a 5-10 cm thin layer at a depth of 12m at the Bangombé site. There are more than twenty drill-holes to investigate the Bangombé natural fission reactor, but only three drill holes, BA145, BAX03 and BAX08, have intersected the reactor (Fig. 1B). The Bangombé reactor has been affected by hydrothermal alteration (Bros et al., 1994; Toulhoat et al., 1994), because it is found at a shallow depth and as thin layer, while the Oklo reactors are more massive and at deeper depths (Gauthier-Lafaye and Weber, 1989; Gauthier-Lafaye et al., 1996).

The Bangombé site shows different redox conditions above and below the reactor. Because geochemical stability of uraninite largely depends upon the redox conditions, the Bangombé reactor provides a unique opportunity to study the geochemical behavior of fission products released from the uranium matrix in the natural environment. The Franceville basin is the host for the Oklo and the Bangombé uranium deposits and consists of five sedimentary units designated as the FA to the FE layers (Gauthier-Lafaye and Weber, 1989). In the Bangombé region, the FB black shale layer is about 11~12 m in depth and is underlain by the FA basal sandstone (Fig. 1B). Many isotopic studies have been completed to determine the geochemical behavior of fission products released from the natural fission reactors of Oklo and

Bangombé (Loss et al., 1989; Nagy et al., 1991; Gauthier-Lafaye et al., 1996; Hidaka and Holliger, 1998). Most of the fissiogenic REE are well retained in the natural reactors. However, the loss of some amount of light REE (LREE) from the reactors has been recognized from the results of bulk rock analyses (Curtis et al., 1989; Hidaka et al., 1992; Menet et al., 1992). Menet et al. (1992) measured Nd isotopes of the Oklo reactor 10 and the surrounding rocks, and found the released fissiogenic Nd along carbonate-filled fissures in the range of 0.5-1.0 m. Our current interest is to elucidate when and how the fission products have migrated and finally retained. Instrumental development of micro-region analysis by secondary ion mass spectrometry offers great advantages in determining the migration and incorporation processes of fission products into specific minerals. During the past decade, it has been recognized that some of the fission products have been incorporated into specific phases; platinoids elements into metallic aggregates (Holliger, 1991; Hidaka et al., 1993); Rb, Ba, LREE and Pu into apatite (Hidaka et al., 1994; Bros et al., 1996; Horie et al., 2004); LREE into florencite, coffinite and françoisite (Janeczek and Ewing, 1996a; 1996b); LREE and noble gases into Al-phosphate (Dymkov et al., 1997; Meshik et al., 2000). In this paper, in-situ isotopic analysis of Ce, Nd, Sm, Eu, Pb and U were performed on U- and REE-bearing minerals found in the sandstone layer just beneath the Bangombé reactor.

2. EXPERIMENTAL

2.1. Samples

The samples in this study were taken from the BAX03 drill-core. Fig. 2 shows a stratigraphic section of the bore-hole BAX03. The reactor zone in BAX03 drill-core occurs at 11.75-11.80 m depth (about 5 cm thick). Petrologic observation shows that the FB layer that overlays the reactor contains a weathered zone (2.5-8.3 m in depth), an oxidized zone (8.3- 8.8 m) and that fissiogenic elements have migrated from the reactor (11.4-11.75 m). Fissiogenic REE-bearing florencite, $(REE)Al_3(PO_4)_2(OH)_6$, was found 5 cm above the reactor (Janeczek and Ewing, 1996a). On the other hand,

study of the FA sandstone layer has not yet been undertaken. In this study, all the samples were taken from the FA sandstone layer beneath the reactor zone of BAX03 drill-core. Four samples taken from 12.10-12.20 m, 12.20-12.30 m, 12.30-12.50 m, 12.75-13.10 m in depth are identified hereafter as BAX03.1215, 1225, 1240 and 1290, respectively. Prior to in-situ isotopic analysis, mineral observation and identification of all four thin section samples were performed by an electron microprobe (JEOL XA-8200). The samples and their specific mineralogies are listed in Table 1. Among the four thin sections, the samples 1225 and 1290 are the same samples in which REE-bearing françoisite, $(REE)(UO_2)_3O(OH)(PO_4)6H_2O$, and U-enriched goethite, FeOOH were previously discovered, respectively (Janeczek and Ewing, 1996b; Janeczek, 1999). Although mineral observation and chemical analysis of major elements of françoisite and goethite were previously carried out by Janeczek and Ewing (1996b), the isotopic measurements were not performed. Besides the françoisite and goethite, in this study we found several phosphorus coffinite grains in BAX03.1225 and 1240, and uraninite grains in 1215 and 1290 that were subjected for isotopic analyses. In the 1290 sample, micro-uraninite grains observed in an organic aggregate coexist with goethite that is deposited along fractures in sandstone. Backscattered electron images of the minerals those U and REE isotopic compositions were measured in this study are shown in Fig. 3.

2.2. Isotopic Measurements by SHRIMP

Isotopic analyses of the thin section samples were performed by a Sensitive High Resolution Ion Micro-Probe (SHRIMP II) at Hiroshima University. A few nA of O_2^- primary ion beam focused onto a 30 □m diameter spot was used for sputtering the polished section. The mass resolution (M/□M at 1% of peak height) was adjusted to 5500 of the peak by using 80 □m width-source slit and 100 □m width-collector slit for ^{204}Pb, ^{206}Pb, ^{207}Pb, ^{208}Pb, ^{235}U and ^{238}U sequential isotope measurements. For REE measurements M/□M was adjusted to ~8800 by setting 70 □m width-source slit and 40

□m width-collector slit in order to avoid isobaric interferences of oxide and some unknown species onto atomic REE ion peak (Hidaka, 1998; Horie et al., 2004). The masses ^{140}Ce, ^{142}Ce+^{142}Nd, ^{143}Nd, ^{144}Sm+^{144}Nd, ^{145}Nd, ^{146}Nd, ^{147}Sm, ^{148}Nd, ^{149}Sm, ^{150}Sm+^{150}Nd, ^{151}Eu, ^{152}Sm, ^{153}Eu were scanned for REE analyses. Instrumental mass fractionation effect onto raw isotopic data was corrected by comparison of the data between individual samples and standard samples. In this study, NIST610 standard glass and natural uraninite from Faraday Mine (Ontario, Canada) were used as standard materials (hereafter, STD) for REE and U isotopic analyses (Hidaka, 1998; Horie et al., 2004).

3. RESULTS

Isotopic data of Ce, Nd, Sm and Eu in individual minerals are summarized in Table 2. The REE isotopic analysis only for the sample 1215 could not been carried out, because the physical damage of the thin section was found before measurements. Therefore, the data for the sample 1215 are not shown in Table 2. ^{142}Ce isotopic abundance is not directly measured from in-situ ion probe analysis because of the presence of isobaric mass interference from ^{142}Nd. Therefore, in this study, ^{142}Ce abundances were calculated by subtraction of ^{142}Nd values, assuming that the Nd isotopic compositions in individual minerals resulted from simple two-component mixing between non-fissiogenic and fissiogenic isotopes. The data for fissiogenic component can be referred from the previous isotopic study of the Bangombé reactor core BAX03.1180 that was taken from the vicinity of the reactor zone (Hidaka and Gauthier-Lafaye, 2000). For the calculation, ^{142}Nd/^{146}Nd=1.597 and 0.483 were used as isotopic ratios of end-members for non-fissiogenic and fissiogenic components, respectively. The mixing proportions of two components in the individual minerals were estimated from the ^{143}Nd/^{146}Nd ratios. Details of the calculation method are described in section 4.1.2. The calculated ^{142}Nd/^{146}Nd ratios of individual minerals are as follows: BAX03.1225-coffinite=0.714, 1225-françoicite=0.835, 1240-uraninite=

0.586, 1240-coffinite=0.597, 1290-uraninite=1.450. The $^{140}Ce/^{142}Ce$ ratios of individual minerals were calculated after subtraction of ^{142}Nd interferences from ^{142}Ce by using the $^{142}Nd/^{146}Nd$ ratios.

U and Pb isotopic data of the individual minerals are shown in Table 3. The data suggest that mixing of depleted U ($^{235}U/^{238}U<0.00725$) in the reactor with non-depleted U ($^{235}U/^{238}U=0.00725$) in peripheral rocks occurred by dissolution and recrystallization of U-bearing minerals. $^{235}U/^{238}U$ ratios of the minerals showed evidence of migration of depleted U from the reactor. Although U-Pb system of geological samples has been generally used to understand chronological history, the U-Pb data of the Bangombé samples may not provide direct information of the formation of primary and secondary U-bearing minerals because of significant disturbance of U-Pb system that resulted from mixing of radiogenic Pb from depleted U and non-depleted U. However, the assumption of two-component mixing allows us to put temporal constraints on the formation of secondary minerals in association with geochemical alteration near the Bangombé site.

4. DISCUSSION

4.1. Migration of Fissiogenic Ce, Nd, Sm and Eu from the Reactor Core

Fission and neutron capture are main reactions which cause the large isotopic anomalies of the elements in a reactor. Because of the contribution of fissiogenic isotopes, the isotopic ratios of individual minerals are different from non-fissiogenic isotopic data. In the mass region around LREE, fission product yields decrease with the mass number. Among REE isotopes detected in this study, ^{140}Ce, ^{142}Ce, ^{143}Nd, ^{145}Nd, ^{146}Nd, ^{147}Sm, ^{148}Nd, ^{149}Sm, ^{151}Eu, ^{152}Sm, and ^{153}Eu include fissiogenic isotopes. If the samples contain a certain amount of fissiogenic component that originated from the reactor, $^{143}Nd/^{146}Nd$ and $^{145}Nd/^{146}Nd$ ratios in the samples are larger than those of non-fissiogenic values obtained from STD samples. On the other hand, the $^{140}Ce/^{142}Ce$ ratios in the samples are expected to be lower than that of STD, because the fissiogenic

$^{140}Ce/^{142}Ce$ ratios estimated from the fission yields of ^{235}U, ^{238}U and ^{239}Pu, 1.06, 1,27 and 1,09, respectively (England and Rider, 1994), are lower than the non-fissiogenic ratio (7.99). In addition, some of REE isotopes are sensitive to the neutron flux, because they have large neutron capture cross sections. The decrease of the $^{149}Sm/^{147}Sm$ ratio is evidence for neutron capture reactions because of extraordinary large thermal neutron capture cross section of ^{149}Sm (42000 barn).

4.1.1. Chemical fractionation of REE

Remarkably, the isotopic data for individual minerals vary with their distance from the BAX03 reactor. All of the minerals from three sandstone layers BAX03.1215, 1225 and 1240, except 1290 (deepest) show lower $^{235}U/^{238}U$ ratios (0.00588-0.00638) than the normal value (0.00725). If the depletions of ^{235}U were caused by in-situ ^{235}U-fission in the mineral, much larger isotopic deviations of Nd and Sm should be evidenced in the individual minerals (Hidaka and Holliger, 1998; Hidaka and Gauthier-Lafaye., 2000). For comparison, the isotopic data of reactor sample BAX03.1180 are also listed in Table 2. It is evident that the isotopic deviation of BAX03.1180 is much larger than those of other samples analyzed in this study. This suggests that the isotopic variations in the samples from the sandstone occurred by mixing of fissiogenic components released from the reactor with non-fissiogenic components in the original materials.

Figure 4 shows diagrams for isotopic ratios of two different elements, Ce-Nd, Sm-Nd and Eu-Nd, in individual minerals. The data for standard material and the reactor sample BAX03.1180 are also plotted in the same figure. The REE components in the individual minerals resulted from mixing between the two end-members. The diagrams for $^{143}Nd/^{146}Nd$ vs. $^{149}Sm/^{147}Sm$ (Fig. 4B) and $^{152}Sm/^{147}Sm$ vs. $^{153}Eu/^{151}Eu$ (Fig. 4C) show linear correlations, which indicates little chemical fractionation among Nd, Sm and Eu during and after formation of the REE-bearing minerals. On the other hand, the diagram for $^{140}Ce/^{142}Ce$ vs. $^{143}Nd/^{146}Nd$ (Fig. 4A) shows a non-linear correlation,

which suggests large chemical fractionation between Ce and Nd. According to the simple calculation, the elemental abundances of Ce in the individual minerals are approximately 5 times larger than that of Nd. Chemical fractionation between Ce and other REE due to a change of the oxidizing state from Ce^{3+} to Ce^{4+} is often observed under oxidizing conditions such as marine environments. Therefore, this is geochemical evidence that uraninite in the reactor core was once partly dissolved and released fission products from the reactor under the oxidizing conditions, and then the dissolved uranium coprecipitated with non-fissioned uranium that was already present in sandstone.

4.1.2. U and REE differentiation

The proportion of the fissiogenic component (x) relative to the total fraction of individual samples can be calculated by the following equation:

$$R_{meas.} = R_f \cdot x + R_n \cdot (1-x) \qquad (1)$$

where $R_{meas.}$, R_f, R_n are isotopic ratios of sample, fissiogenic component, and non-fissiogenic component, respectively (Hidaka et al., 1988).

For the determination of the proportions, x and (1-x), of Ce, Nd, Sm and Eu in individual samples, $^{140}Ce/^{142}Ce$, $^{143}Nd/^{146}Nd$, $^{149}Sm/^{147}Sm$ and $^{153}Eu/^{151}Eu$ isotopic ratios were used, respectively. The calculation results are listed in Table 4. Note, the proportion of fissiogenic LREE in individual samples decreases with the increase in the distance from the BAX03 reactor.

Although uraninite grains in BAX03.1290 show normal $^{235}U/^{238}U$ ratios (0.00725) within analytical uncertainties, they include fissiogenic LREE. This cannot be explained by simple calculation of two component mixing between reactor and non-fissiogenic materials. A previous study of REE isotopes of the Bangombé reactor showed that the elemental abundances of non-fissiogenic REE in the Bangombé RZ are very low (ΣREE<500 ppm) in spite of its high U concentration (29.5-45.0 wt.%) (Hidaka and Gauthier-Lafaye, 2000). In addition, REE patterns (Hidaka and Gauthier-

Lafaye, 2000) and mineralogical observation (Janeczek and Ewing, 1996b; Jensen and Ewing, 1998) suggest that uraninite in the Bangombé RZ has been partially dissolved and affected by supergene alteration. In particular, Stille et al. (2003) described the enrichment of LREE in groundwater that passes through the Bangombé uranium deposit. Fissiogenic REE was probably released by the dissolution of uraninite in the RZ, and then reprecipitated with U as phosphate minerals. During the processes from uraninite dissolution to precipitation of phosphate minerals, chemical fractionation may have occurred between U and REE because of different capacities of these minerals to incorporate REE (Dymkov et al., 1997). Thus, incorporation of fissiogenic LREE occurred in phosphate minerals, even though the amount of ^{235}U depletion is not consistent with the proportion of fissiogenic component calculated from two component mixing. Because the REE contents of the sandstone are very low (□REE=16.4 ppm for BA145 sandstone; Hidaka and Gauthier-Lafaye, 2000), migration of fissiogenic REE is sensitively detected as isotopic anomalies even if the absolute amounts of migrated isotopes are small. Therefore, it can be concluded that the addition of reactor-generated nuclides to BAX03.1290 uraninite is the cause of the isotopic anomalies for Ce, Nd and Sm, despite the presence of non-depleted $^{235}U/^{238}U$.

4.2. Chronological Information from Pb Isotopes

We have endeavoured to obtain chronological information of dissolution of reactor uraninite and fixation of fissiogenic LREE in the secondary minerals. In order to address this issue, Pb-isotopic compositions of individual minerals were measured. Pb-isotopic compositions of the secondary minerals do not directly provide chronological record because of the disturbance of U-Pb systems due to alteration, but these data do allow us to deduce key information on the formation ages of individual secondary minerals that are related to the timing of dissolution and/or precipitation of the uraninite. As shown in Table 3, U and Pb isotopic ratios in the same minerals and at the same depth of sandstone are remarkably homogeneous. This also suggests that

such minerals formed after the mixing of reactor uraninite with the original minerals in the sandstone. If the radiogenic Pb-isotopes in individual minerals have grown since their formation, the formation ages can be calculated from the $^{207}Pb/^{206}Pb$ ratios. However, in this case, Pb-isotopic ratios of individual minerals do not provide direct chronological information because of the disturbance of U-Pb decay system due to the isotopic mixing event.

Figure 5 shows $^{204}Pb/^{206}Pb$ vs. $^{207}Pb/^{206}Pb$ diagram of all of the minerals. The data plots of all minerals give a single line in spite of the variation of U isotopic compositions and the contents of U in the individual minerals. The data suggest that the Pb-isotopes in the individual minerals were derived from recent mixing event of two components, because radiogenic Pb in the individual minerals has not sufficiently grown since the mixing event. It is reasonable to consider that the Pb in the minerals has been supplied from two different end-member phases. One is the original mineral existed in the sandstone, and the other is the fissiogenic nuclides produced in the reactor. From a determination of Pb isotopic signature of the end-members shown in Fig. 5, chronological information can be deduced.

4.2.1. Original materials

BAX03.1290 goethite and uraninite show the highest $^{207}Pb/^{206}Pb$ ratios (0.131-0.134). The uraninite grains contain non-depleted U in spite of the incorporation of significant amounts of fissiogenic LREE. Mineralogical observations show that the goethite was formed by aqueous alteration (Janeczek, 1999). Collomorphic goethite aggregate in fractures of the sandstone BAX03.1290 show overgrown rims. According to Janeczek (1999), U distribution in the goethite suggests oscillatory adsorption of U during the crystal growth of the iron oxyhydroxide. Assuming no contribution of radiogenic Pb due to the decay of depleted ^{235}U, a formation age of the original uraninite can be calculated from the $^{207}Pb/^{206}Pb$ ratios after correction of common Pb from ^{204}Pb abundance. Table 5 shows the calculated formation ages of goethite and uraninite.

The isotopic compositions of Pb extensively trapped in the altered zircon found in the sandstone of Bangombé were used for the correction of common Pb, because the most likely source of the Pb is considered to be the surrounding 2 Ga-old uranium deposit (Mathieu et al., 2001). The data provide formation ages from 2.02 to 2.08 Ga which are comparable to the U-Pb age of 2.05±0.03 Ga from the uraninite of the Oklo ore deposit (Gancarz, 1978). Apparently, the old ages calculated from $^{207}Pb/^{206}Pb$ of the goethite and uraninite may be interpreted as the time of the migration of relict radiogenic Pb from the 2.05 Ga-old uraninite as a result of recent dissolution. The Pb isotopic data suggest that the BAX03.1290 uraninite was precipitated from the detritus of 2.5 Ga-old uraninite in the sedimentary rocks by recent alteration.

4.2.2. A timing of migration of fissiogenic isotopes in association with dolerite dyke intrusion

Assuming that the Pb isotopic compositions of the individual minerals can be simply discussed by using a two component mixing model, Pb isotopic growth in the secondary minerals should provide evidence of an igneous event at the Bangombé site. The extrapolation of the Pb correlation line to $^{207}Pb/^{206}Pb$-axis in Fig. 5 indicates the correction of common Pb included into the secondary minerals. The intercept provides a $^{207}Pb/^{206}Pb=0.0531 \pm 0.0012$. Since depleted ^{235}U materials in this site are considered to originate from the reactor, the $^{235}U/^{238}U$ ratio of another end-member (reactor material) can be fixed at 0.005855 based on the data for BAX03.1180 (Hidaka and Gauthier-Lafaye, 2000). The two values, $^{207}Pb/^{206}Pb=0.0531$ and $^{235}U/^{238}U= 0.00585$, give an age 0.798 ± 0.045 Ga. This age corresponds to the timing of dolerite dyke intrusion event in this area, ranging between 0.53 and 1.00 Ga (Bonhomme et al., 1982). This event is well known as a major thermal episode that caused major loss of Pb from uraninite at the Oklo site (Gauthier-Lafaye et al., 1996). On the other hand, geochronological studies of the Bangombé site remain insufficient, although it is expected that the Bangombé deposit has also been affected by a similar thermal episode

as at the Oklo site. The most reliable age for dolerite dyke intrusion event, 0.860 ± 0.040 Ga is provided by U-Pb analysis of two zircon crystals from the dolerite (Zetterström, 2002). Our Pb age of 0.798 ± 0.045 Ga is consistent with the zircon U-Pb data within the analytical error.

4.3. Comparison of the Alteration History of the Oklo and Bangombé Deposits

We have previously discussed the differences between the alteration processes of the Oklo and Bangombé reactor zones as determined from the chemical differentiation of U and REE in uraninite taken from the various kinds of reactor zones (Hidaka and Gauthier-Lafaye, 2000). There are significant differences in the U-REE differentiation observed in non-altered Oklo reactor zones (SF84 at zone 10 and SD37 at zone 10), altered Oklo reactor zones (Front 305 at zone 9), and Bangombé reactor zone (BA145, BAX03 and BAX08). The different correlation slopes between U and REE in individual reactor zones is a result of the different geochemical processes and environments for uraninite alteration.

It is interesting to compare our Pb data with other Pb data in order to understand the alteration history at the Oklo and Bangombé areas, because more significant chemical differentiation between U and Pb is expected than that in the U and REE differentiation. Figure 6 shows a diagram for $^{204}Pb/^{206}Pb$ vs. $^{207}Pb/^{206}Pb$ of the Oklo samples. The other data are from reactor zones 10, 13 and peripheral uraninite with normal U outside of the reactors at the Oklo deposit (Gancarz, 1978; Gauthier-Lafaye et al., 1996). For comparison, our Pb data obtained are also plotted in Figure 6. The data show different trends possibly due to the differences in the alteration processes of individual uraninites. Samples SF42 and SD37 are from the Oklo reactor zones 10 and 13, respectively. Since both of the reactor zones are located at 310 m and 230 m deep underground, respectively, they have not been affected by weathering. In addition, samples from SD37 were disturbed by hydrothermal alteration due to intrusion of dolerite dyke, because they located only 15 m from the dolerite dyke in the Oklo

deposit. Thus geological conditions are reasonably reflected for the Pb isotopic compositions as follows. The low ^{204}Pb contents of the samples are evidence for no contamination of Pb from the reactors as a result of weathering. $^{207}Pb/^{206}Pb$ ratios in samples from SD37 are significantly lower than those of SF42, which reflect a greater mobilization of Pb from the uraninite due to the dolerite dyke intrusion.

Besides ^{235}U-depleted samples, uraninites outside of the reactors, ES24 and another 10 samples (open circles and open countertriangles, respectively, in Fig. 6) also provide meaningful Pb isotopic signatures related to geological events. Evidence of U-Pb isotopic disturbance is revealed in sample ES24 located deep underground and 50 m from the dolerite dyke (Gauthier-Lafaye et al., 1996). As shown in Fig. 6, the data for ES24 show low ^{204}Pb abundance, and are plotted close to the end-member of the two-component mixing line of BAX03 data measured in this study. Furthermore, the $^{207}Pb/^{206}Pb$ ratios of ES24 are in the range of those of SD37 and BAX03.1215-coffinite grains. The similarity of the Pb isotopic data also suggests that Pb was significantly mobilized in ES24, SD37 and BAX03 in association with the intrusion of dolerite dyke. On the other hand, the data points represented by open countertriangle in Fig. 6 have a slope. All 10 samples are considered to have been affected by recent alteration, because they are located near the surface of the Oklo deposits. Although the data are scattered in Figure 6, possibly due to mixing of other components during alteration, they are clearly affected by the dolerite dyke intrusion event.

5. CONCLUSION

SHRIMP analyses of individual U-bearing minerals in the sandstone layers beneath the Bangombé reactor provide isotopic evidence for the migration of fissiogenic LREE from the reactor associated with supergene alteration. The geochemical history of the Bangombé site can be simply and reasonably explained by a model of two-component mixing between reactor-generated nuclides and the original minerals with non-fissiogenic isotopes. Systematic analytical results for the Ce, Nd,

Sm and Eu isotopic data show chemical fractionation between U and LREE during the formation of the secondary minerals due to alteration. The proportion of fissiogenic LREE in the individual minerals decreases with an increase in the vertical distance from the BAX03 reactor. Large chemical fractionation, especially observed between Ce and other LREE, suggests that the secondary minerals were formed under oxidizing conditions.

Pb isotopic analyses do not directly provide information on the timing of individual mineral formation. However, the systematic Pb isotopic data may be recognized using a two-component mixing model between the 2.05 Ga-old original uraninite and fissiogenic material from the reactor as end-members. In addition, Pb-data suggest that the fissiogenic material as an end-member was formed from reactor component in association with thermal activity due to dolerite dyke intrusion approximately 0.798 Ga ago, and then mixed with 2.05 Ga-old uraninite minerals during recent alteration.

Acknowledgements

This study was financially supported by visiting research fellowship program from Japan Society for the Promotion of Science (S99095 to J.J. and S03748 to FGL). RCE thanks the Science & Technology Program of the Office of Civilian Radioactive Waste Management for partial support. We thank Y. Shibata for his help with SEM work. Critical reading and comments by A. Meshik (Washington Univ., U.S.A.), J.R. DeLaeter (Curtin Tech. Univ., Australia) and an anonymous journal reviewer were helpful to improve the first draft of this paper. The suggestions from the Associate Editor , B. Marty were useful in revising the manuscript.

REFERENCES

Bodu R., Bouzigues H., Morin N., Pfiffelmann J.P. (1972) Sur l'existence d'anomalies isotopiques rencontrées dans l'uranium du Gabon. C.R. Acad. Sci. Paris 275, 1731-1734.

Bonhomme M., Gauthier-Lafaye F., and Weber F. (1982) An example of Lower Proterozoic sediments: The Francevillian in Gabon. Precam. Res. 18, 87-102.

Bros R., Gauthier-Lafaye F., Larqué P., Samuel J., and Stille P. (1994) Mobility of uranium, thorium, and lanthanides around the Bangombé natural nuclear reactor (Gabon). Proc. XVIII Intl. Symp. Sci. Basis Nucl. Waste Management, 1187-1194.

Bros R., Carpena J., Sera V., and Beltritti A. (1996) Occurrence of Pu and fissiogenic rare earth elements in hydrothermal apatites from the fossil natural nuclear reactor 16 of Oklo (Gabon). Radiochim. Acta 74, 277-282.

Curtis D.B., Benjamin T.M., Gancarz A.J., Loss R.D., Rosman K.J.R., De Laeter J.R., Delmore J.E. and Maeck W.J. (1989) Fission product retention in the Oklo natural fission reactors. Appl. Geochem. 4, 49-62.

Dymkov Y., Holliger P., Pagel M., Gorshkov A., and Artyukhina A. (1997) Characterisation of a La-Ce-Sr-aluminous hydroxy phosphate in nuclear zone 13 in the Oklo uranium deposit (Gabon). Min. Depos. 32, 617-620.

England T.R. and Rider B.F. (1994) Evaluation and compilation of fission product yields 1993. LA-SUB-94-170.

Gancarz A.J. (1978) U-Pb age (2.05×10^9 years) of the Oklo uranium deposit: In Natural Fission Reactors. IAEA, Vienne, pp513-520, TC-119/40.

Gauthier-Lafaye F. and Weber F. (1989) The Francevillian (lower Proterozoic) uranium ore deposits of Gabon. Econ. Geol. 84, 2267-2285.

Gauthier-Lafaye F., Holliger P., and Blanc P.-L. (1996) Natural fission reactors in the Franceville basin, Gabon: A review of the conditions and results of a critical event in a geological system. Geochim. Cosmochim. Acta 60, 4831-4852.

Hidaka H., Masuda A., Fujii I., and Shimizu H. (1988) Abundance of fissiogenic and

pre-reactor natural rare-earth elements in a uranium ore sample from Oklo. Geochem. J. 22, 47-54.

Hidaka H., Konishi T., and Masuda A. (1992) Reconstruction of cumulative fission yield and geochemical behavior of fissiogenic nuclides in the Oklo natural reactors. Geochem. J. 26, 227-239.

Hidaka H., Shinotsuka K., and Holliger P. (1993) Geochemical behaviour of ^{99}Tc in the Oklo natural fission reactors. Radiochim. Acta 63, 19-22.

Hidaka H., Takahashi K., and Holliger P. (1994) Migration of fission products into micro-minerals of the Oklo natural reactors. Radiochim. Acta 66/67, 463-468.

Hidaka H.(1998) Isotopic analyses by using a Sensitive High Resolution Ion Micro-Probe (SHRIMP) for natural analogue study of Oklo and Bangombé natural fission reactors. Radiochim. Acta, 82, 327-330.

Hidaka H. and Holliger P. (1998) Geochemical and neutronic characteristics of the natural fossil fission reactors at Oklo and Bangombé (Gabon). Geochim. Cosmochim. Acta 62, 89-108.

Hidaka H. and Gauthier-Lafaye F. (2000) Redistribution of fissiogenic and non-fissiogenic REE, Th and U in and around natural fission reactors at Oklo and Bangombé, Gabon. Geochim. Cosmochim. Acta 64, 2093-2108.

Holliger P. (1991) Systematique U-Pb et etude isotopique in situ ^{235}U-produits de fission de la zone de reaction hybride SF29 (zone 10). Autres zones d'interet sur le site d'Oklo pour les etudes futures. CEA-DTA-CENG, Note Technique DEM No.18/91.

Horie K., Hidaka H. and Gauthier-Lafaye F. (2004) Isotopic evidence for trapped fissiogenic REE and nucleogenic Pu in apatite and Pb evolution at the Oklo natural reactor. Geochim. Cosmochim. Acta 68, 115-125.

Janeczek J. and Ewing R. (1996a) Florencite-(La) with fissiogenic REEs from a natural fission reactor at Bangombé, Gabon. Amer. Mineral. 81, 1263-1269.

Janeczek J. and Ewing R. (1996b) Phosphatian coffinite with rare earth elements and

Ce-rich françoisite-(Nd) from sandstone beneath a natural fission reactor at Bangombé, Gabon. Mineral. Mag. 60, 665-669.

Janeczek J. (1999) Mineralogy and geochemistry of natural fission reactors in Gabon. In: Uranium: Mineralogy, Geochemistry and the Environment (Edited by Burns P.C. and Finch R.) Reviews in Mineralogy 38, 321-392.

Jensen K.A. and Ewing R.C. (1998) Petrography and chemistry of the uranium-bearing phases from the uranium ore-deposit at Bangombé. Proc. 1st EC-CEA workshop on the Oklo-natural analogue Phase II project. Nuclear Science and Technology, EUR 18314EN, 139-159.

Loss R.D., Rosman K.J.R., De Laeter J.R., Curtis D.B., Benjamin T.M., Gancarz A.J., Maeck W.J. and Delmore J.E. (1989) Fission product retentivity in peripheral rocks at the Oklo natural fission reactors, Gabon. Chem. Geol. 76, 71-84.

Mathieu R., Zetterström L., Cuney M., Gauthier-Lafaye F., and Hidaka H. (2001) Alteration of monazite and zircon and lead migration as geochemical tracers of fluid paleocirculations around the Oklo-Okélobondo and Bangombé natural nuclear reaction zones (Franceville basin, Gabon). Chem. Geol. 171, 147-171.

Menet C., Menager M.-T., and Petit J.-C. (1992) Migration of radioelements around the new nuclear reactors at Oklo: Analogies with a high-level waste repository. Radiochim. Acta 58/59, 395-400.

Meshik A.P., Kehm K., and Hohenberg C.M. (2000) Anomalous xenon in zone 13 Okelobondo. Geochim. Cosmochim. Acta 64, 1651-1661.

Nagy B., Gauthier-Lafaye F., Holliger P., Davis D.W., Mossman D.J., Leventhal J.S., Rigali M., and Parnell J. (1991) Role of organic matter in containment of uranium and fissiogenic isotopes at the Oklo natural reactors. Nature 354, 472-475.

Neuilly M., Bussac J., Frejacques C., Nief G., Vendryes G. and Yvon J. (1972) Sur l'existence dans un passé reculé d'une reaction en chaine naturelle de fission, dans le gisement d'uranium d'Oklo (Gabon). C.R. Acad. Sci. Paris 275, 1847-1849.

Stille P., Gauthier-Lafaye F., Jensen K.A., Salah S., Bracke G., Ewing R.C., Louvat D.

and Million D. (2003) REE mobility in groundwater proximate to the natural fission reactor at Bangombé (Gabon). Chem. Geol. 198, 289-304.

Toulhoat P., Gallien J.P., Louvat D., Moulin V., l'Henoret P., Guerin R., Ledoux E., Gurban I., Smellie J.A.T., and Winberg A. (1994) Preliminary studies of groundwater flow and migration of uranium isotopes around the Oklo natural reactors. Radiochim. Acta 66/67, 351-358.

Zetterström L. (2002) Geochronology of the Oklo and Bangombé fossil natural fission reactors: tracing the effects of geological events. Ph.D. thesis, Department of Geology and Geochemistry, Stockholm University.

Table 1. Mineralogy of the thin section samples.

sample No.	depth from the surface*	petrography	specific minerals etc.
BAX03.1215	12.10 - 12.20 m	sandstone	uraninite
BAX03.1225	12.20 - 12.30 m	sandstone	coffinite, françoisite
BAX03.1240	12.30 - 12.50 m	sandstone	coffinite
BAX03.1290	12.75 - 13.10 m	sandstone	goethite, uraninite

*The samples were taken from the BAX03 drill-core. The location of each sample is indicated by the depth from the surface. The Bangombé reactor is located at 11.75-11.80 m (see text and Fig. 1).

Table 2 REE isotopic ratios of individual minerals.

	$^{140}Ce/^{142}Ce$	$^{143}Nd/^{146}Nd$	$^{145}Nd/^{146}Nd$	$^{149}Sm/^{147}Sm$	$^{152}Sm/^{147}Sm$	$^{153}Eu/^{151}Eu$
BAX03.1225						
coffinite-1	3.048 ± 9	1.102 ± 10	0.7364 ± 54	0.4903 ± 29	1.021 ± 11	1.141 ± 20
françoicite-1	3.229 ±12	1.116 ± 3	0.7637 ± 29	0.4795 ± 14	1.005 ± 3	1.169 ± 3
françoicite-2		1.106 ± 4	0.7571 ± 21	0.4918 ± 16	1.025 ± 4	1.167 ± 3
BAX03.1240						
uraninite	4.249 ± 12	0.9187 ± 85	0.6273 ± 32	0.6120 ± 39	N.A.	N.A.
coffinite	4.032 ± 9	0.9279 ± 41	0.6294 ± 29	0.6118 ± 28	N.A.	N.A.
BAX03.1290						
uraninite-1	5.277 ± 20	0.8130 ± 30	0.5518 ± 15	0.8045 ± 30	N.A.	N.A.
uraninite-2	5.353 ± 15	0.8089 ± 49	0.5492 ± 30	0.8050 ± 60	N.A.	N.A.
uraninite-3	5.153 ± 17	0.8188 ±40	0.5515 ± 21	0.8003 ± 57	N.A.	N.A.
uraninite-4	5.449 ± 19	0.8066 ±45	0.5485 ± 19	0.8022 ± 54	N.A.	N.A.
STD						
NIST610	7.988 ± 98	0.7076 ± 18	0.4822 ± 13	0.9216 ± 9	1.783 ± 6	1.089 ± 4
uraninite	7.942 ± 86	0.7089 ± 37	0.4826 ± 16	0.9180 ± 45	N.A.	N.A.
BAX03.1180*						
uraninite	2.209	1.464	1.025	0.1010	0.3646	1.230
BAX03.1175**						
florencite		0.9536 ± 33	0.6608 ± 24	0.2938 ± 29		

Analytical uncertainties given for the last digit indicated are 2□ of the mean. N.A.= not analyzed in this study

*The data from Hidaka and Gauthier-Lafaye (2000)

**The data from Janeczek and Ewing (1996a)

Table 3 U and Pb isotopic data of individual minerals in the sandstone samples from BAX03.

	$^{204}Pb/^{206}Pb$	$^{207}Pb/^{206}Pb$	$^{208}Pb/^{206}Pb$	$^{235}U/^{238}U$
BAX03.1215				
uraninite-1	0.000154 ± 3	0.07552 ± 23	0.007262 ± 71	0.00635 ± 10
uraninite-2	0.000225 ± 3	0.08763 ± 12	0.010851 ± 33	0.00606 ± 5
uraninite-3	0.000224 ± 1	0.08552 ± 24	0.010092 ± 64	0.00630 ± 1
BAX03.1225				
coffinite-1	0.0000493 ± 45	0.06056 ± 63	0.02058 ± 100	0.00612 ± 7
coffinite-2	0.0000601 ± 22	0.05736 ± 36	0.02066 ± 74	0.00609 ± 7
coffinite-3	0.0000572 ± 21	0.06484 ± 34	0.02021 ± 66	0.00616 ± 2
coffinite-4	0.0000639 ± 29	0.07068 ± 25	0.02191 ± 32	0.00616 ± 2
coffinite-5	0.0000727 ± 35	0.06753 ± 26	0.03238 ± 80	0.00616 ± 2
coffinite-6	0.0000753 ± 47	0.07208 ± 24	0.02610 ± 52	0.00619 ± 3
coffinite-7	0.0000511 ± 18	0.05522 ± 22	0.01802 ± 42	0.00617 ± 3
françoisite-1	0.000286 ± 3	0.09912 ± 9	0.01267 ± 5	0.00638 ± 3
françoisite-2	0.000320 ± 7	0.09953 ± 23	0.01375 ± 23	0.00631 ± 3
françoisite-3	0.000304 ± 7	0.09925 ± 14	0.01331 ± 13	0.00637 ± 2
BAX03.1240				
coffinite-1	0.000304 ± 3	0.1044 ± 1	0.01358 ± 4	0.00588 ± 2
coffinite-2	0.000337 ± 5	0.1065 ± 2	0.01502 ± 13	0.00588 ± 2
coffinite-3	0.000299 ± 2	0.1021 ± 2	0.01345 ± 4	0.00592 ± 2
BAX03.1290				
goethite-1	0.000484 ± 4	0.1348 ± 2	0.02173 ± 4	0.00722 ± 3
goethite-2	0.000507 ± 3	0.1344 ± 1	0.02169 ± 4	0.00721 ± 3
goethite-3	0.000507 ± 4	0.1344 ± 2	0.02164 ± 3	0.00724 ± 2
goethite-4	0.000511 ± 5	0.1339 ± 5	0.02138 ± 9	0.00726 ± 2
goethite-5	0.000493 ± 4	0.1340 ± 1	0.02168 ± 3	0.00725 ± 3
uraninite- 1	0.000490 ± 9	0.1333 ± 4	0.02117 ± 10	0.00722 ± 3
uraninite- 2	0.000500 ± 5	0.1340 ± 2	0.02142 ± 4	0.00725 ± 3
uraninite- 3	0.000487 ± 3	0.1312 ± 3	0.02063 ± 10	0.00719 ± 5
uraninite- 4	0.000488 ± 5	0.1323 ± 8	0.02101 ± 10	0.00722 ± 3
uraninite- 5	0.000504 ± 6	0.1336 ± 2	0.02140 ± 8	0.00726 ± 3
uraninite- 6	0.000501 ± 6	0.1337 ± 2	0.02139 ± 7	0.00729 ± 3
uraninite- 7	0.000507 ± 3	0.1350 ± 4	0.02182 ± 9	0.00727 ± 10
uraninite- 8	0.000503 ± 8	0.1351 ± 1	0.02182 ± 4	0.00720 ± 10
uraninite- 9	0.000494 ± 3	0.1329 ± 3	0.02115 ± 8	0.00732 ± 10
uraninite-10	0.000502 ± 5	0.1337 ± 3	0.02129 ± 8	0.00729 ± 3

Analytical uncertainties given for the last digit indicated are 2□ of the mean.

$^{235}U/^{238}U$ isotopic ratios for normal (STD) and reactor core (BAX03.1180) are 0.00725 ± 5 (in this study) and 0.005855 ± 3 (Hidaka and Gauthier-Lafaye, 2000), respectively.

Table 4. Proportions of fissiogenic REE components (%) relative to the total (fissiogenic + non-fissiogenic) components in the minerals.

	Ce	Nd	Sm	Eu	U
BAX03.1225					
coffinite	85	52	54	37	76-83
françoicite	82	54	55	57	62-67
BAX03.1240					
uraninite	63	28	38	N.A.	N.A.
coffinite	67	29	38	N.A.	95-100
BAX03.1290					
uraninite	42-47	12-15	14	N.A.	<4
BAX03.1175*					
florencite		33	77		

*The data from Janeczek and Ewing (1996a)

Table 5 Pb isotopic ratios and Pb-Pb ages of goethite and uraninite from BAX03.1290.

	$^{207}Pb/^{206}Pb$	corrected $^{207}Pb/^{206}Pb$	Age (Ma)
goethite-1	0.1348±2	0.1283±11	2075±13
goethite-2	0.1344±1	0.1276±8	2065±10
goethite-3	0.1344±2	0.1276±10	2065±13
goethite-4	0.1339±5	0.1271±13	2058±18
goethite-5	0.1340±1	0.1274±10	2062±13
uraninite-1	0.1333±4	0.1267±24	2053±32
uraninite-2	0.1340±2	0.1273±13	2061±18
uraninite-3	0.1312±3	0.1246±8	2024±12
uraninite-4	0.1323±8	0.1258±15	2040±21
uraninite-5	0.1336±2	0.1269±15	2055±21
uraninite-6	0.1337±2	0.1270±15	2057±21
uraninite-7	0.1350±4	0.1282±8	2074±12
uraninite-8	0.1351±1	0.1284±20	2076±28
uraninite-9	0.1329±3	0.1263±8	2047±11
uraninite-10	0.1337±3	0.1270±13	2057±18

$^{206}Pb/^{204}Pb$=18.61 and $^{207}Pb/^{204}Pb$=15.75 obtained from the average values of galena inclusions in the altered zones of zircon in the FA sandstone of Bangombé (Mathieu et al., 2001) were used for the correction of common Pb.

Figure captions

Fig. 1 Geological setting of the Bangombé area. (A) Geological map of the Franceville basin. (B) Location of bore-holes and Bangombé reactor. Only three bore-holes, BA145, BAX03 and BAX08 intersect the reactor zone.

Fig. 2 Stratigraphic section of the BAX03 drilling-core. The core of the reactor zone is at a depth of 11.75-11.80 m.

Fig. 3 BSE images of typical minerals measured in this study. (A) Françoisite grain of BAX03.1225. (B) Coffinite grain (bright white area) with a few mm of françoisite rim (gray) in quartz of BAX03.1225. (C) Coffinite grain (bright white areas) with clay parts (dark gray) in quartz matrix of BAX03.1240. (D) Collomorphic goethite aggregate in a fracture of BAX03.1290. (E) Micro-sized uraninite in organic aggregate of BAX03.1290. Scale bar in each photo is 50 □m.

Fig. 4 Two-component mixing curves between non-fissiogenic (STD) and fissiogenic materials (reactor) for (A) $^{140}Ce/^{142}Ce$ vs. $^{143}Nd/^{146}Nd$, (B) $^{149}Sm/^{147}Sm$ vs. $^{143}Nd/^{146}Nd$, and (C) $^{153}Eu/^{151}Eu$ vs. $^{143}Nd/^{146}Nd$. Isotopic ratios of STD and reactor in each diagram correspond to those of standard uraninite and Bangombé reactor BAX03.1180, respectively. "f" values in the figure (A) show chemical differentiation factors of Ce relative to Nd. The curve for "f=5" means that the abundances of Ce are 5 times larger than those of Nd in individual minerals. Analytical errors are included in the symbols.

Fig. 5 $^{204}Pb/^{206}Pb$ vs. $^{207}Pb/^{206}Pb$ diagram of the secondary minerals taken from a sandstone layer of the BAX03 drilling-core. Analytical errors are included in the symbols.

Fig. 6 $^{204}Pb/^{206}Pb$ vs. $^{207}Pb/^{206}Pb$ diagram of various kinds of samples from Oklo and Bangombé. The data except BAX03 (●) are cited from previous studies; altered zircon data (×) from Mathieu et al. (2001), ES24 out of the reactors (▲), SD37 of RZ

13 (□), SF42 of RZ 10 (△), GL3535 of RZ 9 (○) are from Gauthier-Lafaye et al. (1996); The samples peripheral to the reactors (▽) are from Gancarz (1978). Analytical errors are included in the symbols.

Fig. 1A

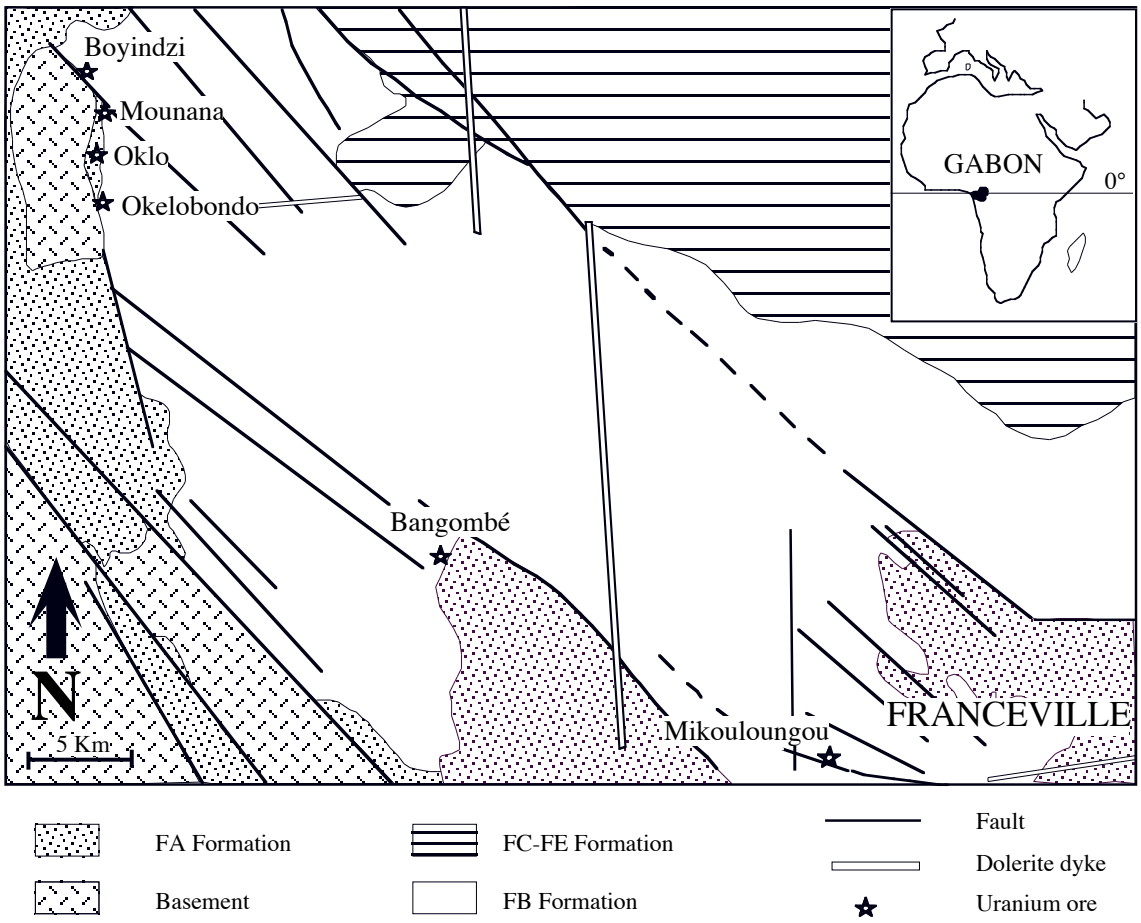
Boyindzi
Mounana
Oklo
Okelobondo
Bangombé
Mikouloungou
FRANCEVILLE
GABON
0°
N
5 Km
FA Formation
Basement
FC-FE Formation
FB Formation
Fault
Dolerite dyke
Uranium ore

Fig. 1B

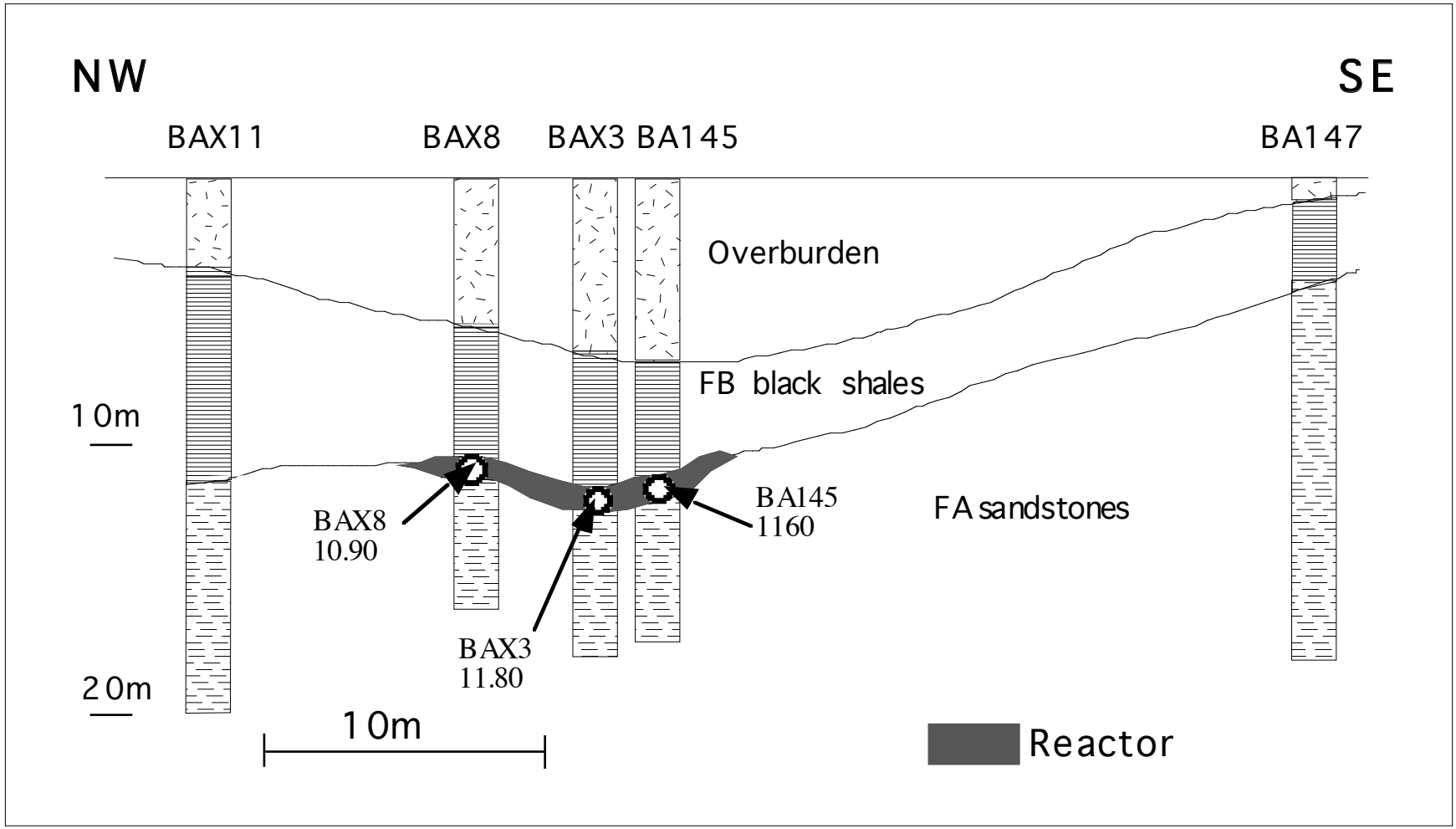
NW
SE
BAX11
BAX8
BAX3
BA145
BA147
Overburden
FB black shales
FA sandstones
10m
20m
BAX8
10.90
BAX3
11.80
BA145
1160
10m
Reactor

BAX3

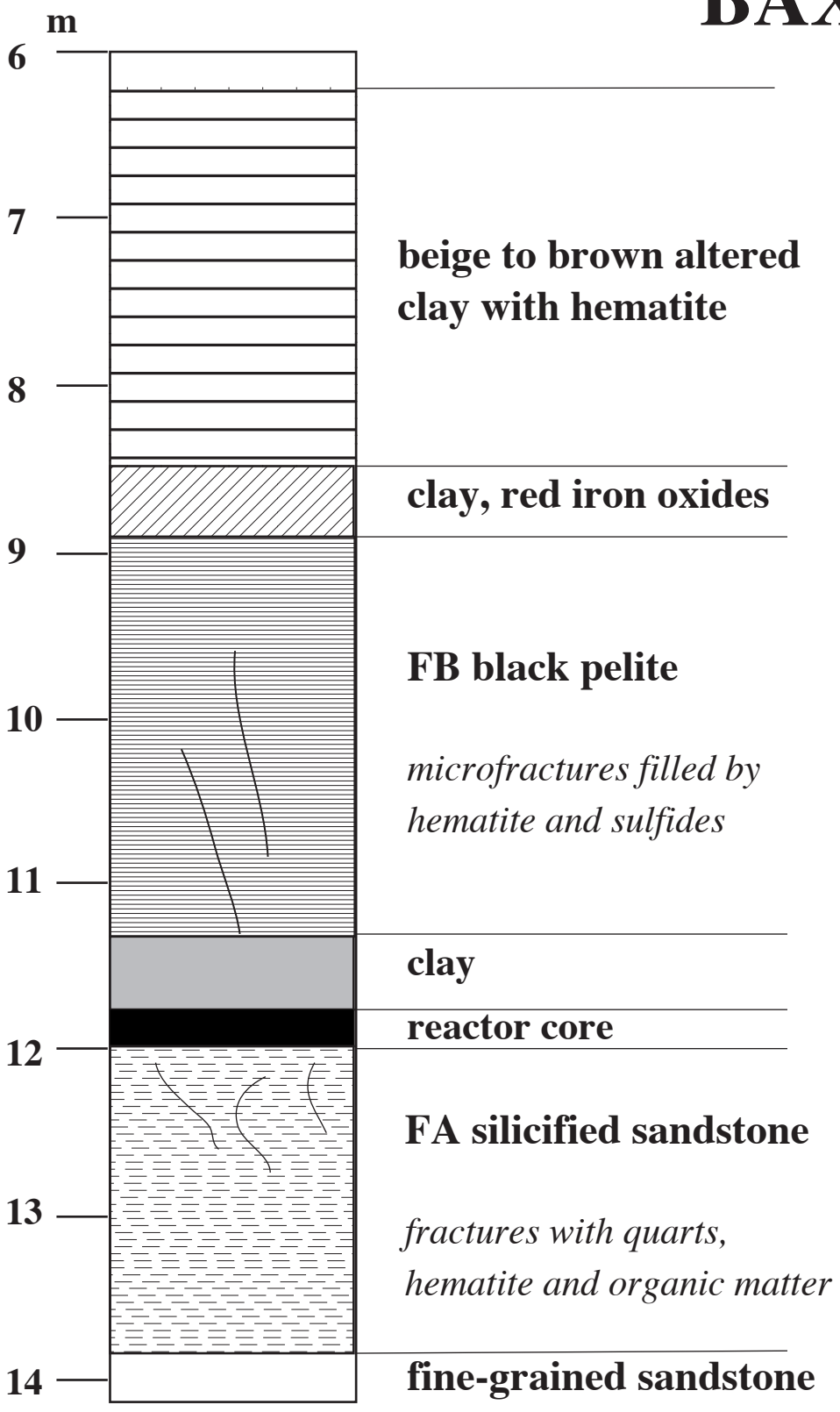
m
6
7
8
9
10
11
12
13
14
beige to brown altered clay with hematite
clay, red iron oxides
FB black pelite
microfractures filled by hematite and sulfides
clay
reactor core
FA silicified sandstone
fractures with quarts, hematite and organic matter
fine-grained sandstone

Fig. 3

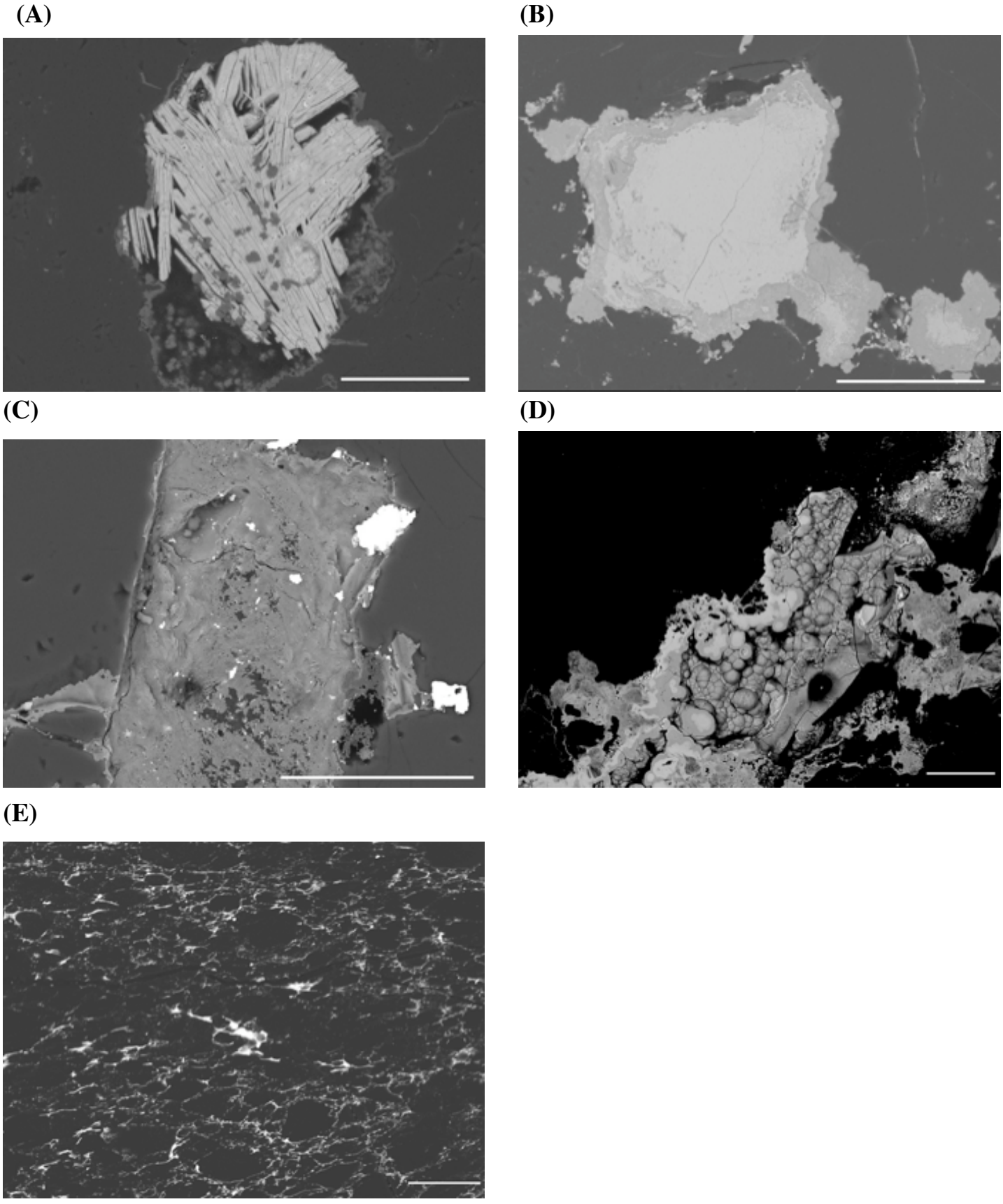

Fig. 4

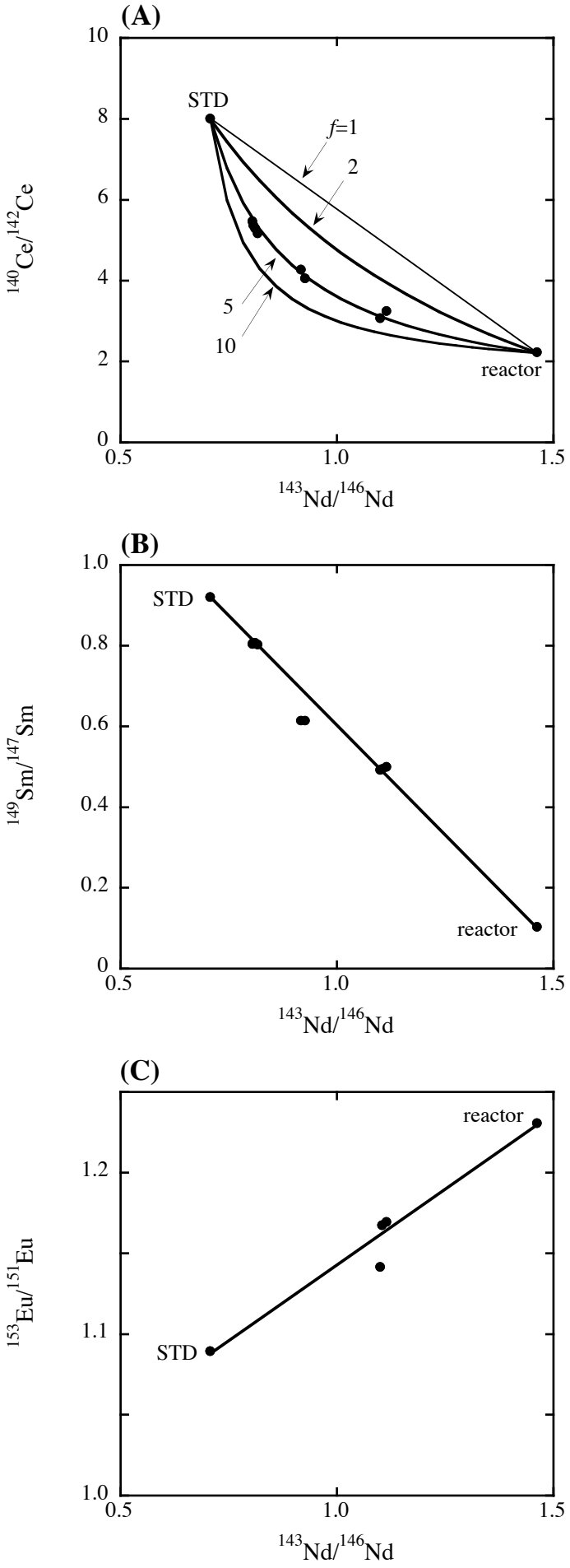
(A)
STD
f=1
2
5
10
reactor
$^{140}Ce/^{142}Ce$
$^{143}Nd/^{146}Nd$
(B)
STD
reactor
$^{149}Sm/^{147}Sm$
$^{143}Nd/^{146}Nd$
(C)
reactor
STD
$^{153}Eu/^{151}Eu$
$^{143}Nd/^{146}Nd$

Fig. 5

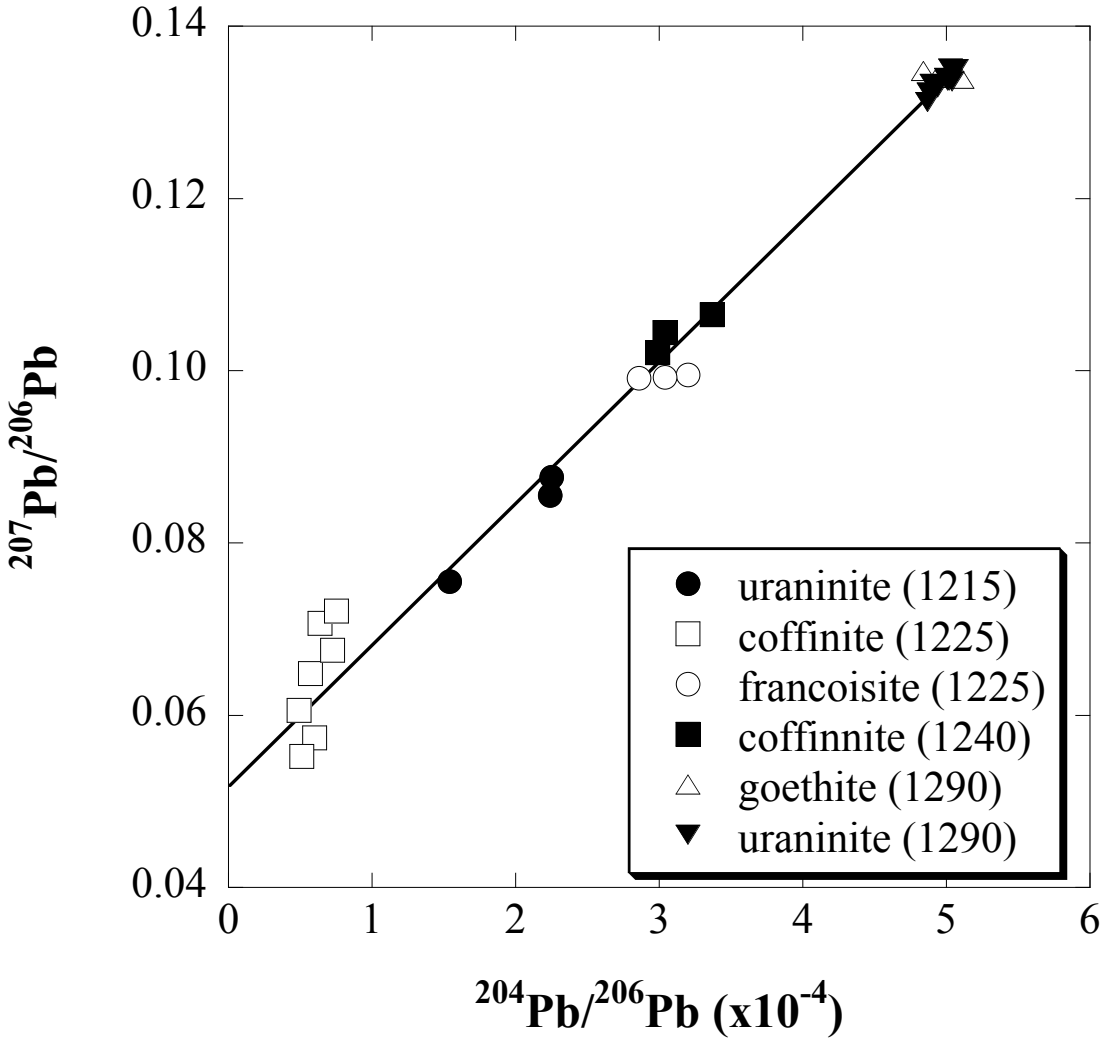
0.14
0.12
0.10
0.08
0.06
0.04
0
1
2
3
4
5
6
$^{207}Pb/^{206}Pb$
$^{204}Pb/^{206}Pb$ (x10^{-4})
uraninite (1215)
coffinite (1225)
francoisite (1225)
coffinnite (1240)
goethite (1290)
uraninite (1290)

Fig. 6

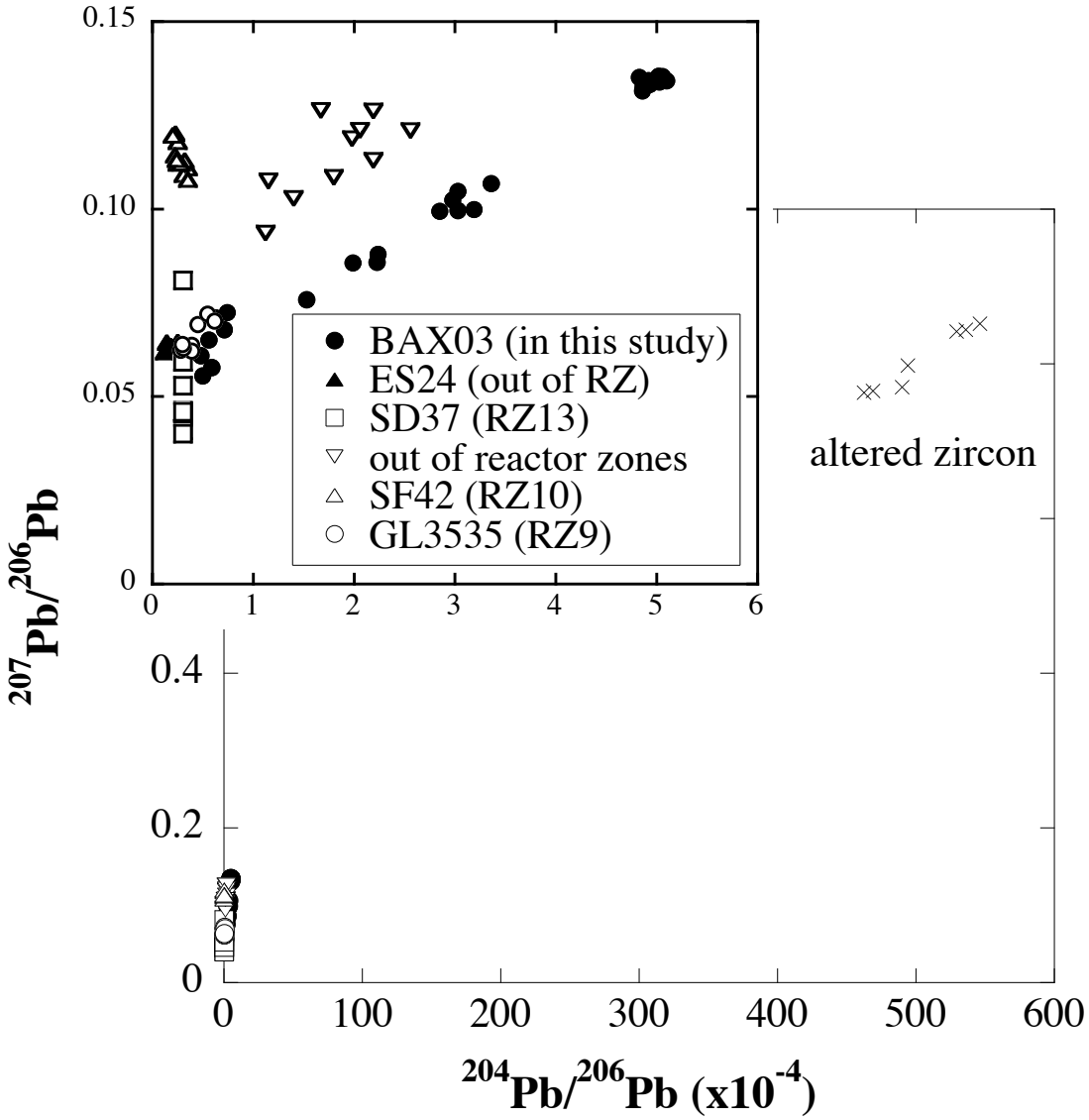
0.15
0.10
0.05
0
0
1
2
3
4
5
6
BAX03 (in this study)
ES24 (out of RZ)
SD37 (RZ13)
out of reactor zones
SF42 (RZ10)
GL3535 (RZ9)
altered zircon
0.4
0.2
0
0
100
200
300
400
500
600
$^{207}Pb/^{206}Pb$
$^{204}Pb/^{206}Pb$ (x10^{-4})